Post-translational Modifications Differentially Affect IgG1 Conformation and Receptor Binding*⑤

Damian Houde‡§¶, Yucai Peng‡, Steven A. Berkowitz‡, and John R. Engen§¶‖

Post-translational modifications (PTMs) can have profound effects on protein structure and protein dynamics and thereby can influence protein function. To understand and connect PTM-induced functional differences with any resulting conformational changes, the conformational changes must be detected and localized to specific parts of the protein. We illustrate these principles here with a study of the functional and conformational changes that accompany modifications to a monoclonal immunoglobulin γ1 (IgG1) antibody. IgG1s are large and heterogeneous proteins capable of incorporating a multiplicity of PTMs both *in vivo* and *in vitro*. For many IgG1s, these PTMs can play a critical role in affecting conformation, biological function, and the ability of the antibody to initiate a potential adverse biological response. We investigated the impact of differential galactosylation, methionine oxidation, and fucosylation on solution conformation using hydrogen/deuterium exchange mass spectrometry and probed the effects of IgG1 binding to the FcγRIIIa receptor. The results showed that methionine oxidation and galactosylation both impact IgG1 conformation, whereas fucosylation appears to have little or no impact to the conformation. FcγRIIIa binding was strongly influenced by both the glycan structure/composition (namely galactose and fucose) and conformational changes that were induced by some of the modifications.   *Molecular & Cellular Proteomics 9:1716–1728, 2010.*

The structure of many proteins can be altered by post-translational modifications (1). Although the impact of post-translational modifications (PTMs)[1] on protein structure is more understood for some modifications (*e.g.* phosphorylation; see Ref. 2), it is less defined for other PTMs and in many cases is protein-dependent. Because there are many important downstream effects of PTMs, including changes in protein localization, protein and cellular diversification, protein functionality, protein stability, protein life cycle, and so forth, understanding how PTMs alter protein structure for as many proteins as possible in a timely manner is a highly desirable goal. Furthermore, in an age where recombinant proteins are being used to treat disease, it becomes ever more important to understand how particular modifications may alter the structure and eventually the function of therapeutic proteins. To realize these goals, methods that permit access to conformational information for modified forms of therapeutic proteins must be developed and refined. In this report, we will illustrate how MS can contribute to structural proteomics by describing our recent work with a recombinant monoclonal antibody (an IgG1), which represents an important class of therapeutic proteins.

Many biopharmaceutical companies are pursuing antibody drugs (3). In particular, the IgG1 subclass of antibodies has evolved into a commonly used therapeutic option for the treatment of a wide range of diseases. IgG1s consist of a dimer of identical heavy chains and light chains that fold to form (from N to C terminus) the variable, CL, CH1, CH2, and CH3 domains (as an example, see Ref. 4). Individual domains are structurally stable and are primarily composed of antiparallel β-sheets arranged in an immunoglobulin-like β-sandwich (5). The variable, CL, and CH1 domains are collectively referred to as the Fab (fragment antigen binding) portion of IgG1, which is responsible for recognizing a specific antigen. The CH2 and CH3 domains together are referred to as the Fc (fragment crystallizable) portion, which carries out effector functions such as binding to Fcγ receptors. These effector functions are essential to many therapeutic antibodies, especially when antibody-dependent cell-mediated cytotoxicity and complement-dependent cytotoxicity are involved in the mechanisms of action (6).

As a biopharmaceutical, IgG1 monoclonal antibodies are critically monitored throughout production (7). In many cases, the impact of structural modifications in these and other formulated versions of biopharmaceuticals are not well understood at a functional level. In the case of IgG1s, with over 1300 amino acid residues and a molecular mass approaching 150 kDa, a large array of PTMs can be incorporated both *in vivo* (during cellular synthesis) and *in vitro* (as a result of handling and processing steps that occur during purification, vialing, and storage). Commonly monitored PTMs on IgG1s

[1] The abbreviations used are: PTM, post-translational modification; DSC, differential scanning calorimetry; H/DX, hydrogen/deuterium exchange; IgG1, immunoglobulin γ1; UPLC, ultraperformance LC.

include methionine oxidation, asparagine and glutamine de-amidation, N-terminal acetylation or cyclization, glycation of lysine, and variable glycosylation (8). Some of these modifications affect only a small percentage of the protein product, and their presence may not change overall outcome. Others, however, can have significant impact on the structure, function, and biological activities of a protein that can involve self-association as well as interactions with other proteins (9). The same PTMs can affect different IgG1 molecules in different ways or have no effect(s) at all. Therefore assessing the presence of PTMs, determining the relative level of the modifications, and understanding the structural effects of PTMs are all important during development of protein biopharmaceuticals.

Two commonly studied IgG1 modifications are methionine oxidation and glycosylation, each of which has been shown to affect biological function (6, 10). Methionine oxidation has been implicated in protein stability (inducing aggregation), and increased oxidation levels have been shown to provoke an immunogenic response (11–13). Elevated levels of methionine oxidation in an IgG1 were shown to impact neonatal Fc receptor (FcRn) and protein A binding (10). Variable glycosylation (*i.e.* different levels of sialic acid, galactose, fucose, or high mannose structures) is known to influence thermal stability and effector functions (14–16). Previous studies have shown that removal of fucose from the glycan present on the Fc portion of an IgG1 can greatly enhance Fc binding to FcγRIIIa, but removal of the entire glycan nearly abolishes FcγRIIIa binding (17). As oxidation and changes to the glycan are both common IgG1 modifications, we were interested in determining the conformational effects of oxidation, afucosylation, and galactosylation and correlating any conformational changes that were observed with changes of FcγRIIIa binding activity.

Conformational analysis of large proteins like antibodies, however, is not trivial. Traditional biophysical techniques such as circular dichroism, DSC, and fluorescence provide useful information, but these techniques look at the entire protein and provide only a global view (18). NMR and x-ray crystallography can both provide high resolution structural analysis, but each is faced with limitations that often make the study of an intact IgG1 difficult or nearly impossible (19–21). Recently we described how hydrogen/deuterium exchange (H/DX) MS could be used to study the conformation and conformational dynamics of an intact IgG1 with resolution down to stretches of several amino acid residues (22). For the present work, we used H/DX MS to study the impact of galactosylation, oxidation, and afucosylation on the conformation and dynamics of an intact IgG1. We also studied the complex of IgG1 and FcγRIIIa to map the points of interaction and probe any changes in the dynamics of the IgG1 as a result of FcγRIIIa interaction. Finally, we correlated the functional activity of all the proteins that were studied by H/DX MS with the observed conformational disturbance(s). Such correlations are impor-tant to connect structure with function and to understand whether a particular PTM is something that may affect the therapeutic value of a recombinant protein.

EXPERIMENTAL PROCEDURES

All chemicals were purchased from Sigma-Aldrich/Fluka unless otherwise noted. Detergent-free β(1–4)-galactosidase and peptide:*N*-glycosidase F were purchased from Prozyme (San Diego, CA). UDP-α-D-galactose was purchased from Calbiochem. Guanidine HCl, tris(2-carboxyethyl)phosphine hydrochloride, and TFA were obtained from Pierce. Hydrogen peroxide (30%) was acquired from Acros (Morris Plains, NJ).

IgG1 Antibodies—The fucosylated and afucosylated recombinant monoclonal IgG1 antibodies and soluble FcγRIIIa receptor (CD16) were produced in Chinese hamster ovary cells and purified by Biogen Idec, Inc. The native IgG1 and eight different variants (see Table I) were produced: deglycosylated, degalactosylated, hypergalactosylated, afucosylated, afucosylated-degalactosylated, afucosylated-hypergalactosylated, oxidized, and hypergalactosylated-oxidized. The afucosylated version of the IgG1 was produced in a cell line having a deficiency in the ability to add fucose to the oligosaccharide chain. A summary of the preparation of the other variants is described here, whereas an expanded discussion can be found in the supplemental data and supplemental Figs. S1 and S2. Creation of deglycosylated, degalactosylated, and afucosylated-degalactosylated IgG1 variants was through incubation of native material with ~100 milliunits of peptide:*N*-glycosidase or β(1–4)-galactosidase for 20 ± 2 h at pH 7.2 and 6.0, respectively, at 37 °C. Hypergalactosylated and afucosylated-hypergalactosylated IgG1 variants were prepared by incubation with ~300 milliunits of galactosyltransferase, 1 mg of UDP-α-D-galactose, and 20 mM MnCl$_2$ at pH 7.2 for 20 ± 2 h at 37 °C (23). Oxidation was achieved by incubating antibody in 0.1% H$_2$O$_2$ for 6 h at ambient temperature followed by the addition of 1 mg of methionine before purification (24). The hypergalactosylated-oxidized IgG1 was prepared with a combination of the procedures mentioned above. All IgG1 variants were purified by size exclusion chromatography using a TSKgel G3000SW$_{XL}$ column (Tosoh Bioscience, San Francisco, CA). The separation was achieved under isocratic conditions at 0.5 ml/min with IgG1 buffer (50 mM sodium phosphate, 100 mM NaCl, pH 6.0). The antibodies eluted at ~18 min, several minutes away from any impurities. IgG1 monomers were collected at 20% peak height, and samples were concentrated to ~3 mg/ml using a 10,000 molecular weight cutoff Amicon Biomax centrifugal concentrator. The native IgG1 (~16% galactosylation) was treated and purified similarly. Antibody concentrations were calculated from the absorbance measured at 280 nm and the theoretical molar extinction coefficient of $\varepsilon = 218,292$ M^{-1} cm^{-1} (25). Successful creation of all forms was verified by mass spectrometry as described in the supplemental data and supplemental Figs. S1 and S2.

Cell-based Apoptosis Assay—The IgG1 analyzed here binds to a membrane receptor (antigen) on the surface of lymphoma cells, causing apoptosis. Based on this mechanism of action, we designed the following cell-based assay to measure the biological activity of the IgG1 variants. A lymphoma cell line, SKW6.4, with high level expression of the receptor antigen was purchased from ATCC and grown in RPMI 1640 medium supplemented with 10% fetal bovine serum. IgG1 molecules were serially diluted and added to cell culture medium together with a cross-linking goat anti-human IgG-Fc secondary antibody from Jackson ImmunoResearch Laboratories (West Grove, PA). Cells were incubated for 72 h, and IgG1-induced apoptosis was measured using a luminogenic substrate that is specific for caspase 3 or 7 (Caspase-Glo 3/7, Promega). Cleavage of the substrate by activated caspase 3 or 7 (apoptotic cells) yields a quantitative luminescent signal that is directly proportional to the level of apoptosis.

TABLE I
Properties of IgG1 variants used in this study
Methionine oxidation was confined to the IgG1 Fc fragment as detailed in supplemental Fig. S2.

IgG1 variant	Glycan composition	Relative percent galactosylation	Relative percent fucosylation	Relative percent Fc oxidation
Native	$Man_3(GlcNAc)_4Gal_1Fuc_1$	~16	>99	<3
Deglycosylated	None	0	0	<3
Degalactosylated	$Man_3(GlcNAc)_4Fuc_1$	<1	>99	<3
Hypergalactosylated	$Man_3(GlcNAc)_4Gal_2Fuc_1$	>99	>99	<3
Afucosylated	$Man_3(GlcNAc)_4Gal_1$	~16	<1	<3
Afucosylated-degalactosylated	$Man_3(GlcNAc)_4$	<1	<1	<3
Afucosylated-hypergalactosylated	$Man_3(GlcNAc)_4Gal_2$	>99	<1	<3
Methionine-oxidized	$Man_3(GlcNAc)_4Gal_1Fuc_1$	~16	>99	>99
Methionine-oxidized-hypergalactosylated	$Man_3(GlcNAc)_4Gal_2Fuc_1$	>99	>99	>99

Caspase 3/7 activation by the IgG1 variants was compared with that of unmodified native IgG1 and reported as percentage of relative potency.

FcγRIIIa Binding Assay—IgG1-Fc binding to FcγRIIIa was assessed using a competitive binding assay based on AlphaScreen technology from PerkinElmer Life Sciences (26). This method uses three reagents: GSH-coated donor beads, GST-tagged FcγRIIIa, and native IgG1-coated acceptor beads. FcγRIIIa is conjugated to donor beads through GSH-GST interaction. Binding of IgG1 to FcγRIIIa brings the donor and acceptor beads into proximity, enabling energy transfer and light production at 520–620 nm. IgG1 variants compete with native IgG1 on acceptor beads for binding to FcγRIIIa, leading to a decrease of fluorescent signal (binding strength is inversely proportional to the measured signal). The three reagents were incubated along with various concentrations (serial 1:2 dilution) of IgG1 variants in a 96-well plate format at 22 $\pm$ 1 °C for 4 h. Native IgG1 was included in each plate to serve as a standard and control. Signals in the 96-well plates were recorded with an EnVision plate reader (PerkinElmer Life Sciences). Analysis of binding strength was carried out with the statistical software PLA (Stegmann Systems, Rodgau, Germany). The binding strength of modified IgG1 variants was compared with that of unmodified native IgG1, and the relative percent binding or -fold increase in binding (afucosylated samples only) was calculated.

Hydrogen/Deuterium Exchange Mass Spectrometry—Hydrogen/deuterium exchange was performed as described previously (22). The time course for labeling was 10 s and 1, 10, 60, and 240 min. Deuterium labeling was quenched by reducing the pH to 2.6 and lowering the temperature to 0 °C. Quenched samples were digested on line with pepsin, desalted, and separated using a special Waters UPLC system designed for hydrogen/deuterium exchange (27). A 6-min linear acetonitrile gradient (8–40%) was used to separate the peptides; both mobile phases contained 0.1% formic acid. Eluate from the C_{18} column was directed into a Waters QTof Premier mass spectrometer with electrospray ionization and lock mass correction (using Glu-fibrinogen peptide). Mass spectra were acquired from m/z 200 to 1700. Pepsin fragments were identified using a combination of exact mass and MS^E aided by Waters Identity^E software (28). Peptide deuterium levels were determined as described by Weis *et al.* (29) using the Excel-based program HX-Express and other custom macros. Any time deuterium uptake graphs are shown, all data within that graph (for all the variants shown in that graph) were obtained under the most identical conditions possible, usually in the same day using identical buffer and instrumental conditions. No adjustment was made for deuterium back-exchange during analysis, and therefore all results are reported as relative deuterium level (30); therefore, data cannot be compared in terms of absolute deuterium values between experiments in which controls and test samples were obtained sep-

arately. Back-exchange in the instrumental system/conditions described here ranged from 15 to 20%, depending on sequence, as verified with totally deuterated control peptides. Approximately 95% of the IgG1 amino acid sequence was covered by the peptic fragments in these experiments as described previously (22). Each analysis was repeated four times over the course of several months. Based on our observations using repeat injections, we found that the error associated with deuterium level determination was 0.1–0.3 Da (that is, ±0.05–0.15 Da for each data point), similar to that reported elsewhere (31). Therefore, we concluded that reproducible changes in deuterium content greater than 0.5 Da were significant.

For IgG1 and FcγRIIIa H/DX-MS binding experiments, 20 μM IgG1 was incubated with 65 μM FcγRIIIa at ambient temperature for 2 h in 50 mM sodium phosphate, 100 mM NaCl, pH 6.0 (equilibration solution). The volume of the equilibration solution was 50 μl. Based on a K_d of 1 μM, ~98% of the IgG1 was bound under these conditions. To initiate labeling, 1 μl (15 pmol of IgG1, 75 pmol of receptor) of the equilibration solution was diluted into 19 μl of deuterated buffer (50 mM sodium phosphate, 100 mM NaCl in D_2O, pD 6.0). In the labeling solution, ~70% of the native IgG1 was bound to FcγRIIIa. Labeling was quenched at specific times by adding an equal volume of quench buffer (as described above), and the quenched material was analyzed in a manner identical to that of unbound IgG1. Approximately 15 pmol of IgG1 were injected into the mass spectrometer for each time point.

RESULTS AND DISCUSSION

Preparation and Characterization of IgG1 Variants—The comparison study of different variants of IgG1 began by creating homogenous preparations of each form as listed in Table I. Each of these forms was derived from native material by treatment with enzymes, chemical modification, or both. The details of the preparation of each form are found under "Experimental Procedures" and in the supplemental data. We used two separate assays to ascertain the functional impact of each modification. These functional data were critical as they allowed us to make a connection between functional consequences and the changes in deuterium uptake that were measured.

Overall Functionality of Modified IgG1 Variants—To ensure that the modifications within the Fc region did not cause dramatic and detrimental changes overall that would cripple the antigen binding activity and render the antibody completely non-functional, a cell-based apoptosis induction assay

was utilized. Based on the mechanism of action of this particular antibody, this apoptosis assay measures the cellular response upon IgG1 binding to a cell surface antigen. The assay uses a polyclonal goat anti-human IgG1-Fc secondary antibody to cross-link the primary antibody (the monoclonal IgG1 under investigation) to promote apoptosis. Both specific antigen binding to the cell surface and relative structural integrity of the Fc region of the primary IgG1, as recognized by the secondary antibody, are required for apoptosis to occur. The assay is not sensitive to small changes in the Fc region that may alter the Fc binding activity of the molecule (see below). IgG1 variants along with native IgG1 were incubated with a lymphoma cell line (SKW6.4), and caspase 3/7 activities were measured after 72 h. The results demonstrated that all of the modified IgG1 molecules had relative potency equal or similar to that of the native molecule. This suggests that the PTMs on this IgG1 did not grossly alter the antigen binding capability of this IgG1 nor grossly change the Fc regions such that the anti-Fc secondary antibody could not recognize the Fc region.

IgG1-Fc Binding Activity of IgG1 Variants—The interaction between this IgG1 and the Fc receptor FcγRIIIa, although not very strong (K_d ~1 μM), is critical for eliciting antibody-dependent cell-mediated cytotoxicity (32). The interaction is carefully monitored during development and commercialization of this and other IgG1 monoclonal products that bind to Fc receptors. The FcγRIIIa binding strengths of the IgG1 variants formed in this study were tested using a competitive binding assay (see "Experimental Procedures") to determine whether there had been altered Fc receptor binding activity. The data are reported in Fig. 1 as relative percent binding or -fold increase in binding (in the case of afucosylated samples only) using the native IgG1 as the reference.

We immediately observed that complete removal of the glycan almost totally abolished IgG1 binding to FcγRIIIa (Fig. 1*A*). This result has been seen before (33–35), thereby validating our assays. Oxidized IgG1 binding activity was nearly the same as that of the native IgG1, whereas the degalactosylated form had slightly weaker binding to FcγRIIIa (a relative binding value of 83%), similar to what was shown previously (17). Hypergalactosylated IgG1 showed 324% relative binding to FcγRIIIa, and the doubly modified IgG1 that was both hypergalactosylated and oxidized also had higher binding (272% relative binding), suggesting that the galactosylation level positively affects IgG1 binding to FcγRIIIa. The afucosylated IgG1 displayed a 49-fold stronger FcγRIIIa binding than native IgG1 (Fig. 1*B*), consistent with previous reports showing that lack of fucose on the IgG1 significantly improves binding to FcγRIIIa (36, 37). Degalactosylation of the afucosylated IgG1 resulted in a slight decrease in binding strength (from 49- down to 40-fold *versus* native IgG1), whereas hypergalactosylation of the afucosylated IgG1 increased the FcγRIIIa binding 78-fold over the native IgG1. Taken all together, it can be concluded that removal of galactose from the
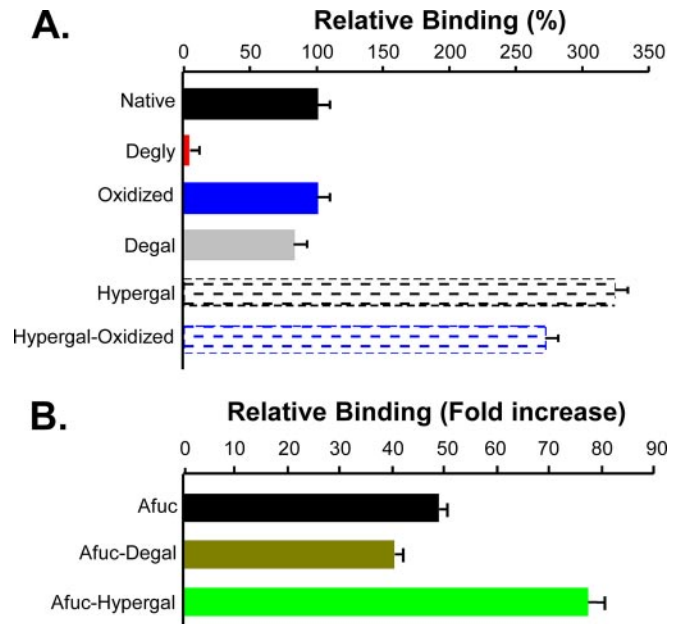

FIG. 1. **FcγRIIIa binding to IgG1.** *A*, relative percent FcγRIIIa binding for each of the forms indicated (see also Table I). All values are relative to the native IgG1. Each IgG1 sample was analyzed six independent times (*n* = 6) with an error less than 10%. *B*, relative -fold increase in FcγRIIIa binding for afucosylated IgG1 variants. All values are relative to the native, fucosylated IgG1 (which if shown would have a value of 0 on this scale). Each IgG1 sample was analyzed six independent times (*n* = 6) with an error less than 5%. Error bars indicate the spread of the 6 determinations *Degly*, deglycosylated; *Degal*, degalactosylated; *Hypergal*, hypergalactosylated; *Afuc*, afucosylated.

IgG1 (irrespective of the presence or absence of fucose) results in consistent and lower FcγRIIIa binding, whereas hypergalactosylation increases FcγRIIIa binding. These results suggest that both fucosylation and galactosylation affect the FcγRIIIa binding capacity of IgG1 and that their effects are additive.

Although the importance of glycans in Fc receptor binding has been demonstrated previously (15–17, 35), it remains unclear how and to what extent the glycans themselves are involved in mediating interactions with the Fc receptor. Krapp *et al.* (38) solved the structure of several glycosylation variants of an IgG1-Fc fragment and concluded that increased galactosylation (corresponding to the hypergalactosylated IgG1 here) led to the greatest spatial distance between CH2 domains in an Fc-only construct. Combined with other reports (14, 16, 35), the authors suggested that increased galactosylation may expose more amino acid residues for binding, thereby increasing FcγRIIIa binding strength. With H/DX MS we were in a position to validate these hypotheses and determine specifically what regions may play a role in conformation-assisted changes to Fc receptor binding. In addition to H/DX MS, we used a number of biophysical methods and compared the results for all of the IgG1 forms that were prepared.

Analysis of Conformational Consequences of PTM—The IgG1 variants generated in this work (with their appropriate control samples) were characterized by a battery of analytical and biophysical methods including LC/MS disulfide mapping, fluorescence, UV spectroscopy, circular dichroism, analytical ultracentrifugation, size exclusion chromatography, DSC, and H/DX MS. Of these, only DSC and H/DX MS detected conformational differences between these IgG1 variants. In the case of DSC, only oxidized and deglycosylated variants showed altered thermograms (see supplemental Fig. S3), consistent with what has been reported previously for the destabilization of the CH2 domain of a deglycosylated (39) or oxidized IgG1-Fc fragment (40). The DSC results are more fully described in the supplemental data. In the case of H/DX MS, results obtained by H/DX MS provided much more insight into what exactly occurs in terms of conformation and conformational dynamics when these PTMs are introduced into this IgG1 and are discussed more fully in the following sections.

H/DX MS of IgG1 Variants—The measurement of backbone amide hydrogen exchange by mass spectrometry has been described previously (30, 41). The folded conformation of a protein can influence the exchange rate at backbone amide positions, particularly in cases where hydrogens bonds are created or destroyed. By measuring hydrogen exchange for the intact protein or for the peptides created after the labeling reaction is quenched, information about protein conformation can be obtained. Anything that perturbs the conformation of a protein, such as PTMs, protein activation, complex formation, etc., may perturb some of the amide hydrogen exchange rates in that protein, allowing one to observe where and to what magnitude conformation has been altered. Unfortunately, this technique does not reveal how side chain conformation may be altered (42). We previously demonstrated that H/DX MS could be used to interrogate the conformational properties of an intact IgG1 antibody (22).

To assess the impact of the IgG1 PTMs used in the current study, we monitored differences in exchange between native IgG1 and each variant (Table I). All of the peptic peptides previously identified for this IgG1 (22) were followed for each variant. There were no significant differences in H/DX between the degalactosylated IgG1 and the native IgG1 (~16% galactosylation; see supplemental Fig. S1). However, when comparing H/DX of hypergalactosylated IgG1 with H/DX in the native or the degalactosylated IgG1 forms, one specific area on the IgG1 molecule was found to exhibit a difference in deuterium incorporation (Fig. 2). All other regions remained unchanged as a result of modification. The area that was changed covered the heavy chain residues ranging from 242 to 254, located in the CH2 domain. The fragment starts as a β-strand, extends to an unstructured region followed by a short α-helix, and ends with a loop in the lower part of the CH2 domain. Pepsin digestion produced >10 overlapping peptide fragments in this region, enabling us to pinpoint which

residues accounted for the altered exchange that was detected. Fig. 2, *A–E*, show the H/DX exchange results of five representative fragments (244–253, 243–254, 242–253, 245–252, and 248–252) in this area. By comparing the exchange data in the many overlapping fragments in the region 242–254 (Fig. 2, *bottom right*), we were able to determine that the primary backbone amide hydrogens responsible for the changes in exchange were those found at residues Leu-243, Phe-244, and/or Lys-247. These backbone NH groups have been highlighted on the structure of the IgG1 shown in Fig. 2*F*. Note that because of the loss of the N-terminal deuterium from peptic peptides (30, 41) we were unable to identify exactly which of the residues (Leu-243, Phe-244, or Lys-247) contains deuterium but were able to exclude the possibility that any deuterium was found in the C-terminal half of the 242–254 region. Comparison of the deuterated native (Fig. 2, *A–E*, *solid black*) *versus* hypergalactosylated (Fig. 2, *A–E*, *dotted black*) forms of the IgG1 revealed that in the hypergalactosylated form these three residues were more protected from exchange. Increased galactosylation protected ~1–3 positions from H/DX. In the deglycosylated IgG1 (Fig. 2, *A–E*, *red curves*), there was more deuterium incorporation in the three residues, implying a loss of hydrogen bonding and/or more solvent exposure. In related experiments, no differences in deuterium incorporation were detected in afucosylated versions of the IgG1, although the differences resulting from the level of galactosylation were preserved in variants that were both afucosylated and differentially galactosylated.

IgG1 that had been oxidized displayed differences in H/DX in only one region when compared with the native protein. This region corresponded to the same heavy chain residues 243–247 that were seen to change as a result of alterations to the glycan. In the oxidized IgG1 (Fig. 2, *A–E*, *solid blue lines*), more deuterium was found in the 243–247 region relative to the native IgG1 (Fig. 2, *A–E*, *solid black lines*). In Met-253 and Met-429, the oxidized sulfurs on each residue are within 5 Å (see supplemental Fig. S2) of one another. The addition of oxygen to each residue likely causes an electrostatic repulsion of the side chains, which is then felt in the conformation of the peptide backbone of residues 243–247. This affect appears to transmit itself over 25 Å from the addition of oxygen to residues Met-253 and Met-429 to the amide hydrogen of Leu-243 and appears to have a destabilizing effect on the IgG1, reducing the backbone amide hydrogen bonding network within residues 243–247 such that more deuterium could be incorporated. The peptide backbone conformation of residues surrounding Met-429 was not influenced (*i.e.* the deuterium incorporation curves were identical) likely because the Met-429 region is stabilized by a rigid antiparallel β-sheet structure, whereas the Met-253 region contains a less stable small α-helix and a loop. It is interesting that addition of oxygen induced a greater destabilizing effect than complete removal of the glycans as indicated by the higher H/DX rates
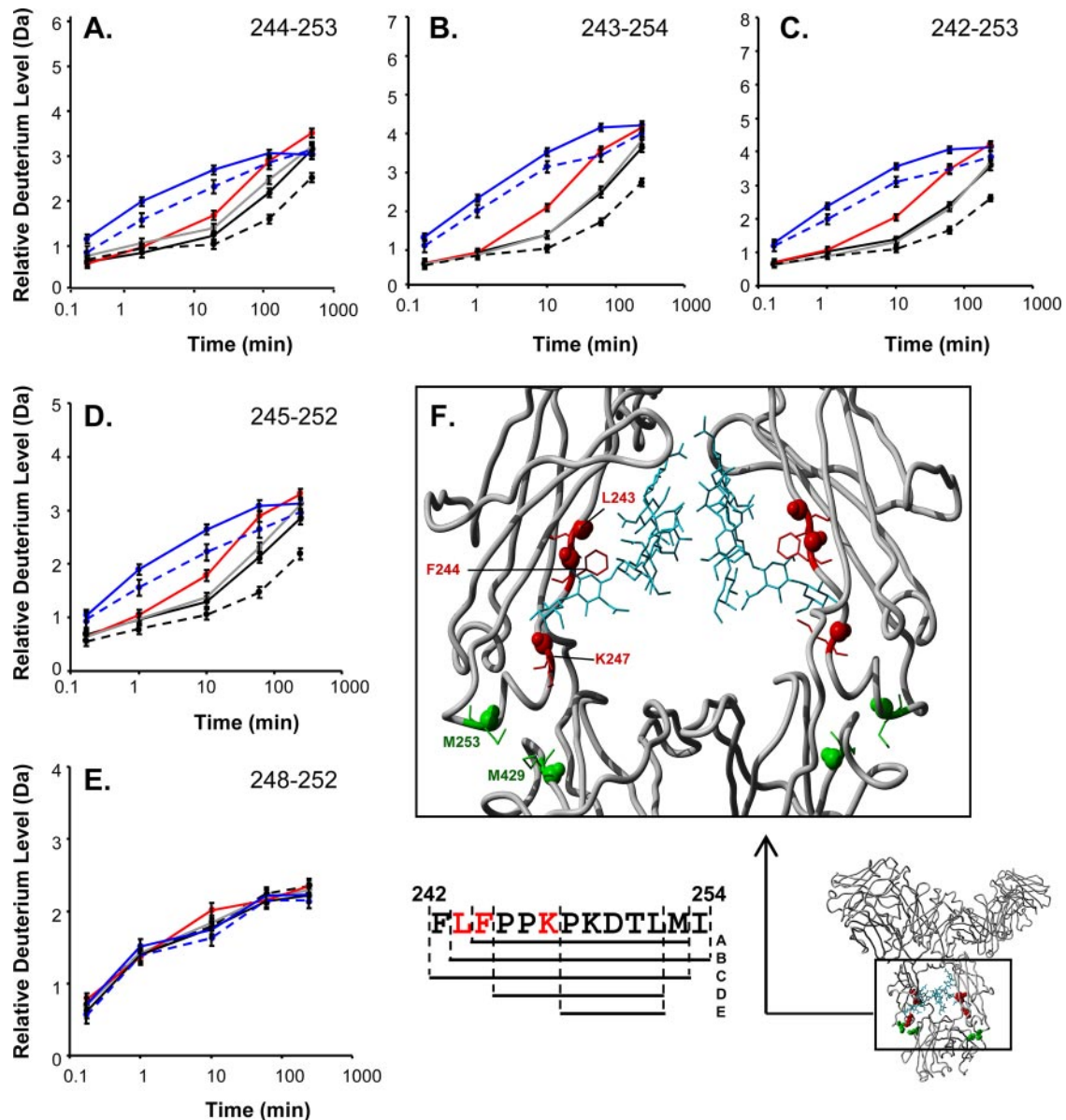
FIG. 2. **Residues 243–247 were affected by PTMs.** *A–E*, the relative deuterium level is shown for five overlapping pepsin fragments covering heavy chain residues 242–254. The level of deuteration was monitored at 10 s and 1, 10, 60, and 240 min for each IgG1 variant. *Solid black*, native IgG1; *solid gray*, degalactosylated IgG1; *dotted black*, hypergalactosylated IgG1; *solid red*, deglycosylated IgG1; *solid blue*, methionine-oxidized IgG1; *dotted blue*, hypergalactosylated-methionine-oxidized IgG1. These traces are an average of four replicates with *error bars* at each time point ranging from ±0.05 to 0.15 Da. The sequence of residues 242–254 is shown at the *bottom* of the figure, and each different peptide (*A–E*) is depicted as a *bar under* the sequence. Note that because the values measured are relative deuterium levels the absolute value of deuterium at each time point cannot be compared with other measurements outside this data set (see "Experimental Procedures"). *F*, a zoomed-in view of the model structure of the IgG1 studied (Protein Data Bank codes 3FZU and 1HZH; see Ref. 22). The *red spheres* indicate the backbone nitrogen and amide hydrogen where the modifications produced differences in deuterium incorporation, and the *green spheres* represent Met-253 and Met-429. Glycans are colored *cyan*.

for oxidized IgG1 than for deglycosylated IgG1. These data suggest that oxidation weakened backbone amide hydrogen bonding and/or solvent protection, whereas galactosylation had the opposite effect. To answer which of these two forces was stronger, we carried out H/DX experiments on a hypergalactosylated and oxidized IgG1 variant. Recall that hypergalactosylation resulted in the least amount of deuteration in this region. However, when the hypergalactosylated species was also oxidized (Fig. 2, *A–E, dotted blue lines*), the exchange curves were much more like those for oxidation alone. Based on these results, we conclude that destabilization of the Fc portion of the IgG1 by oxidation is a stronger destabilizing force than the stabilizing forces from hypergalactosylation.

Bear in mind that in this IgG1 there was essentially no change in receptor binding activity upon oxidation, but there was enhanced receptor binding upon hypergalactosylation (Fig. 1). These results suggest two potential scenarios that are consistent with the receptor binding data. (*a*) The glycans, particularly the terminal galactose, are themselves involved in the interaction with FcγRIIIa, or (*b*) Changes in the glycans cause conformational changes (including those that may not be detected by H/DX MS, such as movement of whole domains while preserving all environments of backbone amide hydrogens), which force the Fc portion into a conformation more amenable to FcγRIIIa binding (a theory proposed by Krapp *et al.* (38)). We favor an interpretation that is somewhat of a combination of both of these models, depending on the change to the glycan.

H/DX MS Data in Light of IgG1-Fc Structures—The first hypothesis that may explain how different PTMs, particularly changes to the glycans, are connected with changes in FcγRIIIa binding is that the receptor actually interacts with the glycans. Crystal structures of an IgG1-Fc fragment in complex with the FcγRIII receptor (not necessarily FcγRIIIa) were solved by Sondermann *et al.* (32) (Protein Data Bank code 1E4K) and Radaev *et al.* (43) (Protein Data Bank codes 1T83 and 1T89) and indicate several points of contact between IgG1-Fc fragment and FcγRIII. Most of the contacts, however, do not involve the glycans but instead involve several hydrogen bonds, hydrophobic contacts, and salt bridges primarily involving residues 235–239 (hinge region), 265–269 (B/C loop), 297–299 (C′/E loop), and 327–332 (F/G loop) of the IgG1-Fc. The structures show the carbohydrate moieties positioned away from the FcγRIII interaction site and not involved in the IgG1-Fc and FcγRIII interaction (with the exception of a minor involvement of the primary GlcNAc on one of the glycan chains, the B chain). So the structural data do not support the hypothesis of direct interaction between glycans and the Fc receptor.

There are structural data supporting the second hypothesis that conformational changes are being induced by changes to the glycans. Yamaguchi *et al.* (17), using NMR and ^{1}H-^{15}N heteronuclear single quantum correlation, compared the hypergalactosylated and degalactosylated IgG1-Fc fragment alone and found chemical shifts associated with Lys-248 (which corresponds to Lys-247 in our IgG1), a residue within the heavy chain 242–254 segment. Investigation of several structures of IgG1-Fc alone and in complex with FcγRIII (particularly Protein Data Bank codes 1E4K and 1FC1 (44)) provides some insight into how galactosylation might cause the differences in deuterium uptake that were observed. Note that although the structure of a hypergalactosylated IgG1-Fc fragment has been solved (Protein Data Bank 1H3V (38)), electron density associated with the α(1–3) arm galactose was lost due to high dynamic motions. Fig. 3 shows a zoomed-in superposition of Protein Data Bank code 1E4K (*red*) and Protein Data Bank code 1FC1 (*blue*) with the glycans in *magenta* and
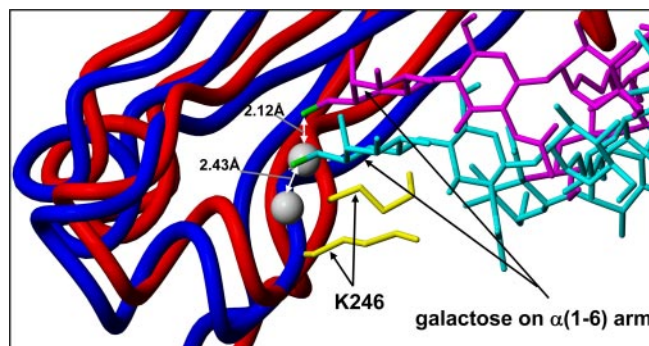

FIG. 3. **Superpositioning of two IgG1-Fc fragment x-ray crystal structures, Protein Data Bank code 1E4K (32) in *red* and Protein Data Bank code 1FC1 (44) in *blue*.** The glycans from Protein Data Bank code 1E4K are *magenta*, and the glycans from Protein Data Bank code 1FC1 are *cyan*. For each protein, the Lys-246 side chain is shown as *yellow sticks* (note that Lys-246 in these structures corresponds to Lys-247 in the IgG1 under investigation). The O6 from galactose (*gal*) on the α(1–6) arm is colored *green*. The backbone amide hydrogen of Lys-246 is shown as a *gray ball*, modeled and positioned with the lowest energy minimization using YASARA software (51). The intermolecular distances between the galactose O6 and the Lys-246 backbone amide hydrogen were measured for each structure, and the values are shown.

cyan, respectively. Lys-246 (in these structures, Lys-246 corresponds to Lys-247 in the IgG1 studied here) in both structures is shown as *yellow sticks*. The terminal galactose on the α(1–6) arm of the glycan has the potential for hydrogen bonding (45) between the O6 oxygen of galactose (Fig. 3, *green*) and the backbone amide hydrogen of Lys-246 (Fig. 3, *gray ball*) with measured distances of 2.12 and 2.43 Å for chain B of 1E4K and 1FC1, respectively (these distances were 2.78 and 2.70 Å for chain A, respectively). If a hydrogen bond formed between the backbone amide hydrogen of Lys-247 and the O6 of galactose (assuming the angles were conducive to a hydrogen bond), it could explain why there is protection from exchange at this lysine in the hypergalactosylated form (relative to the degalactosylated IgG1) because a strong hydrogen bond would protect this position from deuteration. Although intriguing, this model does not rule out that galactosylation has caused a conformational change in the IgG1 nor does it consider that other IgG1-Fc fragment structures indicate the galactose O6-Lys-246 NH distance to be well over 4 Å and much too long for a traditional H-bond.

H/DX MS Analysis of IgG1 and FcγRIIIa Binding—To better clarify how changes to the glycans resulted in changes in receptor binding, we performed H/DX MS experiments on the complex between intact IgG1 and FcγRIIIa. Remember, all residues of the IgG1 were present in contrast to the data gathered from crystals of the complex where only the Fc region of the IgG1 was present. Two independent binding experiments were carried out. First, the intact native IgG1 and FcγRIIIa complex was analyzed, and second, the afucosylated-hypergalactosylated IgG1 and FcγRIIIa complex was analyzed.
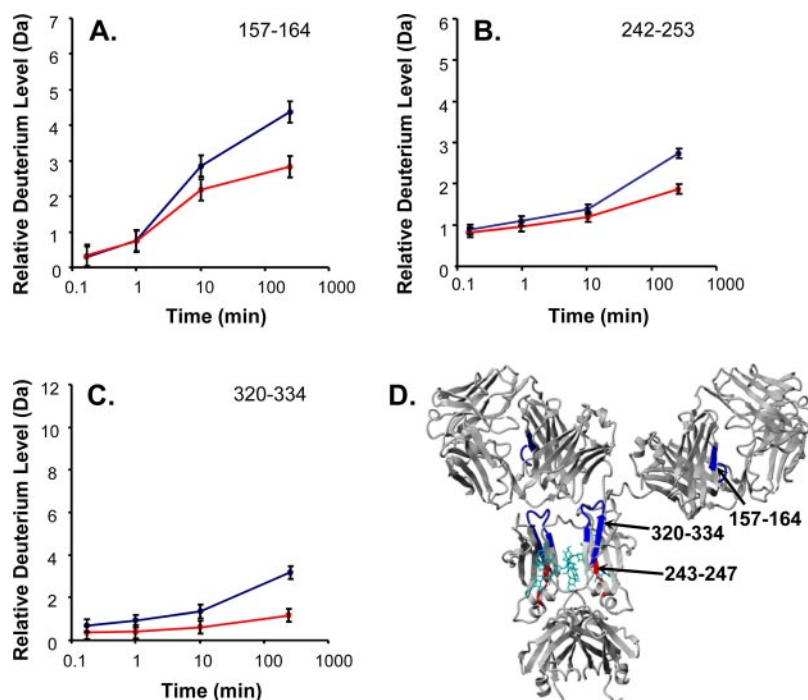
FIG. 4. **Comparison of deuterium levels in native IgG1 and native IgG1 bound to FcγRIIIa.** *A–C*, the relative percent deuteration is shown for three heavy chain peptides, 157–164, 242–253, and 320–334. The level of deuteration was monitored at 10 s and 1, 10, and 240 min for each sample. The *blue* trace is the deuterium level of the IgG1 alone, and the *red* trace is the deuterium incorporation of IgG1 in complex with FcγRIIIa. The experiment was repeated with $n = 2$, and the error for each measurement was ±0.05–0.15 Da. *D*, the structure of the IgG1 as in Fig. 2; glycans are colored *cyan*, and areas of difference from FcγRIIIa interaction are colored *red* or *blue* to correspond with Fig. 6. As in Fig. 2, overlapping peptides covering residues 242–254 allowed us to narrow the region of change to residues 243–247; therefore, those residues are highlighted on this structure.

Because the native IgG1-FcγRIIIa interaction is not very strong ($K_d \sim 1$ μM), a large excess of FcγRIIIa was needed to ensure that the majority of the IgG1 would be bound with FcγRIIIa at any given time (42). Although ideally we would have wanted the IgG1 to be >90% bound at any one time, the lower affinity, large molecular weight, and sample concentrations required were not experimentally feasible (explained in more detail in Ref 42). Our binding experiment resulted in ~70% of the native IgG1 being bound to FcγRIIIa at any one time during deuterium labeling. Native IgG1 and FcγRIIIa were incubated together at ambient temperature for 120 min, and then the exchange was performed in the same manner as for all other experiments in this report. Deuterium incorporation was compared for IgG1 alone and IgG1 in the presence of FcγRIIIa with all experiments being repeated twice. It should be noted that the stoichiometry of the IgG1 and FcγRIIIa is 1:1 and that FcγRIIIa is reported to bind to one half of the IgG1, leaving the other half of the IgG1 unbound (34). Therefore, because the intact IgG1 is a homodimer, the deuterium levels for IgG1 peptides reflect an average of the bound and unbound monomers. When differences in deuterium levels upon binding are observed, they are very likely higher (as much as double) but appear lower due to the contribution of exchange into the unbound heavy chain in the IgG1 homodimer. All peptic peptides from both the IgG1 and the FcγRIIIa proteins

were analyzed, totaling well over 200 peptides. The presence of the receptor had minimal impact on our ability to follow deuterium incorporation in the peptic peptides from the IgG1 (see also supplemental Fig. S4), due mainly to the extremely high efficiency of the UPLC separations. More than 88% of the peptides we detected and followed for IgG1 alone were found and monitored for IgG1 in the presence of FcγRIIIa, and total linear sequence coverage was still obtained for the IgG1 because almost all of the peptides that could no longer be observed in the presence of the receptor came from regions of the IgG1 in which there were redundant and/or overlapping fragments. In native IgG1, three areas were found to exhibit different deuterium exchange profiles in the presence of the receptor. These areas included heavy chain residues 157–164, 243–247, and 320–334, all of which were protected from deuterium incorporation in the presence of the receptor (Fig. 4). Changes in these regions were reproducible in replicate experiments, and overlapping peptides displayed similar behavior, giving us high confidence that the changes observed were real and significant. Residues within fragment 320–334 were identified previously as interacting with FcγRIIIa (32). However, residues 157–164 and 243–247 were not formerly reported to be associated with FcγRIIIa interaction.

In a second set of experiments, using the same experimental conditions as mentioned above, deuterium exchange into
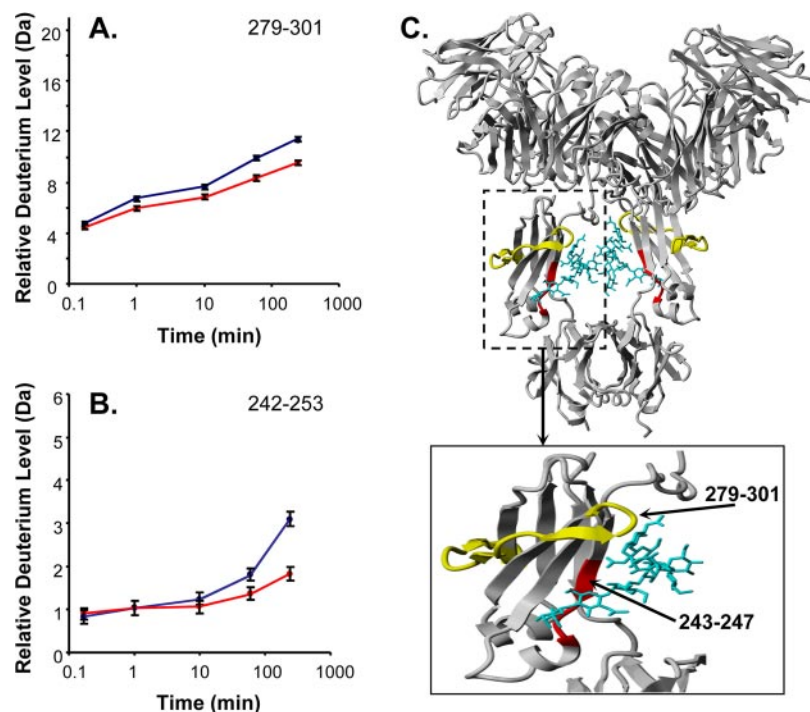
FIG. 5. **Comparison of deuterium levels in afucosylated-hypergalactosylated IgG1 and afucosylated-hypergalactosylated IgG1 bound to FcγRIIIa.** The relative percent deuteration is shown for two heavy chain peptides, 279–301 (*A*) and 242–253 (*B*). The level of deuteration was monitored at 10 s and 1, 10, 60, and 240 min for each sample. The *blue* trace is the deuterium level of the IgG1 alone, and the *red* trace is the deuterium incorporation of IgG1 in complex with FcγRIIIa. The experiment was repeated with $n = 2$, and the error for each measurement was ±0.05–0.15 Da. *C*, the structure of the IgG1 as in Fig. 2; glycans are colored *cyan*, and areas of difference from FcγRIIIa interaction are colored *red* or *yellow* to correspond with Fig. 6. As in Figs. 2 and 4, overlapping peptides covering residues 242–254 allowed us to narrow the region of change to residues 243–247; therefore, those residues are highlighted on this structure.

afucosylated-hypergalactosylated IgG1 in complex with FcγRIIIa was measured. Because afucosylated-hypergalactosylated IgG1 has a significant increase in affinity for FcγRIIIa and much higher activation (Fig. 1*B*), close to 50× more than the native form, a K_d (20 nM) that was 50× lower than that for the native IgG1 complex was used to approximate the relative proportions of bound and free species in the exchange experiment. Based on this K_d in the binding experiment, ~96% of the IgG1 molecules were bound at one time. Comparison of the deuteration of afucosylated-hypergalactosylated IgG1 with and without FcγRIIIa (again well over 200 peptides) resulted in two regions that displayed differences. Residues 279–301 and 243–247 were protected from exchange in the bound state (Fig. 5, *A* and *B*), and both of these areas are located within the CH2 domain of the IgG1 heavy chain (Fig. 5*C*). Changes in residues 243–247 were also seen in the native IgG1-FcγRIIIa interaction (Fig. 4), but changes in residues 279–301 were not seen previously in the binding of native IgG1 with FcγRIIIa. Furthermore, no changes in deuteration were detected in residues 157–164 when receptor bound to the afucosylated-hypergalactosylated IgG1, although changes were seen in residues 157–164 when the receptor bound to native IgG1. The differences observed between the native IgG1 and afucosylated-hypergalactosylated IgG1 binding to FcγRIIIa suggest different modes of interaction.

Data Summary and Interpretation—Based on all of the H/DX data, we have summarized (Fig. 6) how modifications to the IgG1 influence both the conformation and conformational dynamics of the molecule as well as influence receptor binding. When the IgG1 becomes hypergalactosylated, the primary region of alteration in deuterium incorporation is in residues 243–247 (Fig. 6*B*). As described in Fig. 3, this may be the result of changes to the way the sugars interact with amino acids in this part of the CH2 domain. Changes to the CH2 domain as a result of hypergalactosylation influence receptor binding, making the binding higher in affinity (Fig. 1). The exact mechanism that leads to tighter binding is not clear, but the data suggest that it is a conformational change or more likely a combination of changes in conformation and changes in dynamics that together stiffen the region and make deuterium incorporation proceed at a slower rate. This is the same region of IgG1 that was altered upon deglycosylation (22) and oxidation (Fig. 2).

In terms of receptor binding, the native IgG1 and FcγRIIIa form a complex that influences deuterium exchange in several locations (Fig. 6*C*). In addition to the change in exchange in the 243–247 region (the same region shown to be important in hypergalactosylation), changes were seen in residues 320–334 just nearby in the CH2 domain and in residues 157–164 in the CH1 domain, which is very much removed from the CH2
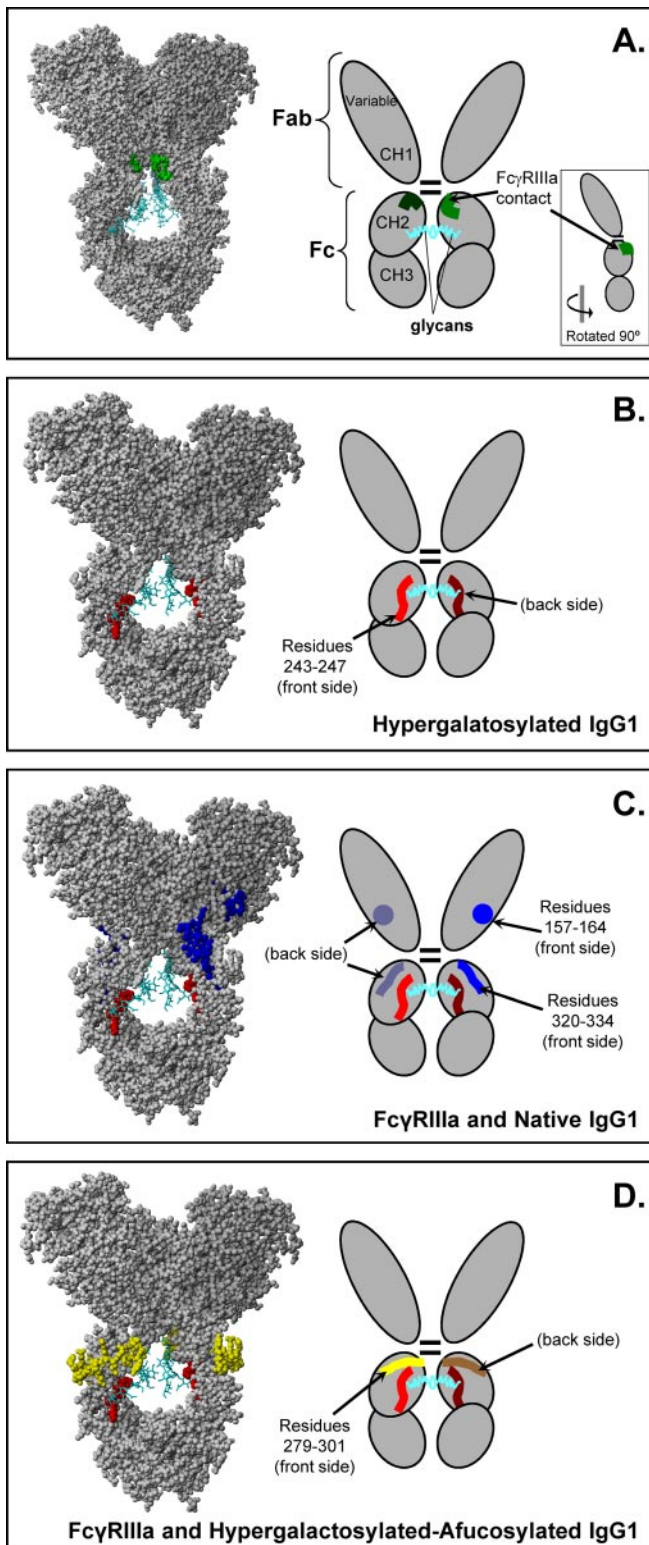
FIG. 6. **Illustration of IgG1 areas affected upon interacting with FcγRIIIa.** A space-filling representation (*left*) and a schematic form (*right*) are shown in each panel. The Protein Data Bank coordinates used to generate the models are the same as those described in Fig. 2. *A*, the location of FcγRIII interaction on the structure of IgG1. Regions of FcγRIIIa receptor contact with the IgG1 are colored *green*

domain. Comparing Fig. 6, *A* and *C*, one sees that the region where the receptor primarily interacts with the IgG1 (based on crystal structures and modeling of receptor binding to Fc regions only) is in the CH2 domain, near enough to influence residues 243–247 and 320–334 almost directly. We hypothesize that the receptor may also have a secondary interaction or contact surface that includes residues 157–164 or that it may occlude this region, thereby causing a reduction in deuterium incorporation in that area. Note that the difference in H/DX is very small at early exchange time points but progressively increases with deuterium incubation time (Fig. 4, *A* and *B*), implying that the reduction in deuterium incorporation is a result of protein dynamics and stability, perhaps involving movement of FcγRIIIa on/off this secondary site in the CH1 domain.

The situation is quite different, however, in the binding between FcγRIIIa and the afucosylated-hypergalactosylated IgG1 (Fig. 6*D*). In that case, the H/DX data indicate that protection is greatest at two regions within the CH2 domain. Again residues 243–247 are influenced, but then a new region, residues 279–301, appears to be influenced by binding (see also Fig. 5, *A* and *B*). Although the changes in deuterium levels here are smaller than in other experiments, the locations where these changes are observed are quite reliable. We saw no changes in deuterium incorporation in the other two regions that were observed to be altered in binding of FcγRIIIa to native IgG1 (157–164 and 320–344). Such results suggest a different mode of binding. It is not surprising that a different binding mode is observed because based on the functional data it is known that the affinity of the receptor for the IgG1 is very much larger in the afucosylated form (Fig. 1*B*). Examining the crystal structure of an IgG1-Fc fragment bound with an FcγRIII receptor (Protein Data Bank code 1E4K) helps to illustrate how the lack of fucose may enhance this interaction. Fucose, although over 7 Å from the nearest FcγRIII residue, interacts with several residues within the IgG1-CH2 domain (particularly in the C′/E loop) (46). These interactions act to stabilize both the glycan core as well as several residues within the CH2 domain. In Fig. 6*D*, we can see that the hypergalactosylated-afucosylated IgG1 exhibits protection in two regions of the CH2 domain (279–301 and 243–247). The 279–301 region contains several residues in the CH2 C′/E loop that are known to interact with fucose. Accordingly, fucose may act as a gate where removal of fucose relaxes

---

based on Refs. 32, 43. *B*, areas where deuterium exchange was altered when the IgG1 became hypergalactosylated. The residues colored *red* (243–247) correspond to those described in Fig. 2. *C*, areas where deuterium exchange was altered when FcγRIIIa bound to native IgG1. Changes were observed in the regions colored *blue* and *red* as described in Fig. 4. *D*, areas where deuterium exchange was altered when afucosylated-hypergalactosylated IgG1 bound to FcγRIIIa. Changes were observed in the regions colored *yellow* and *red* as described in Fig. 5.

the overall structure of both the glycan and regions within the CH2 domain. Thus, an increase in the plasticity in these regions may enable FcγRIIIa to make stronger and or more dynamic contacts with the IgG1. Such a notion, that protein flexibility and dynamics are critical components to protein-protein interactions, has been demonstrated previously (47). To truly understand the implications of all of the glycans on the IgG1 and FcγRIIIa interaction, we would need to study all the IgG1 variants in complex with FcγRIIIa by H/DX MS, something that is beyond the scope of this initial study. Based on the data collected, we favor the hypothesis that changes in protein conformation in the CH2 domain, caused by the removal of fucose, are translated to changes in conformation or conformational dynamics such that the receptor sees a new mode of binding and that residues 243–247 and 279–301 play a key role.

Conclusions—In this work, we investigated the conformational effects of methionine oxidation (heavy chain residues Met-253 and Met-429), fucosylation, and galactosylation on an intact IgG1 antibody. We characterized these IgG1 molecules functionally and observed that these PTMs resulted in very different functional behavior in the IgG1 molecule. We then applied biophysical methods to understand how and why the modifications caused such obvious and different functional properties. Of all the biophysical methods used, H/DX MS was the most revealing and helpful. In particular, it helped us localize the conformational alterations accompanying the modifications to the IgG1 molecule as well as characterize and classify the different modes of receptor binding that resulted. In terms of tools for structural proteomics, H/DX MS is very valuable as we believe our data have illustrated.

Changes to the local environment of heavy chain residues 243–247 of the CH2 domain were involved in almost all the modifications we studied. We (22) and others (40) have previously observed changes in this region. This change in the CH2 domain is in direct proximity to the glycans, and alterations in the glycan structure and composition appear to be able to influence this region. Complete IgG1 galactosylation protected some residues from exchange (relative to the degalactosylated IgG1), probably as a result of interactions between galactose and the protein polypeptide backbone at Lys-247 of the heavy chain. This increase in structural rigidity in this region leads to increased receptor binding. The 243–247 region appears to transmit the information somehow such that binding to Fc receptor is altered, perhaps by changing the relative orientation of the CH2 domain with respect to the CH1 domain (first proposed by Krapp *et al.* (38)). It is also possible that binding in solution is slightly different from in the crystal, and this region is directly involved in the interaction with Fc receptor.

Removal of fucose from the biantennary glycans core produced the strongest affinity of IgG1 for FcγRIIIa, increasing the binding over 49-fold, yet no conformational changes were observed in the IgG1 itself when compared with the native IgG1. Therefore, it seems possible that in this case the glycan itself and/or the effect the glycan has on the orientation of the CH2/CH1 domains is involved more directly in mediating the IgG1 interaction with FcγRIIIa. When fucose was removed, conformational changes such as those seen with hypergalactosylation were not indirectly translated to changes in receptor binding.

H/DX MS revealed several regions of protection in the complex between IgG1 and FcγRIIIa. A different set of protected regions were observed in the afucosylated-hypergalactosylated IgG1 and FcγRIIIa binding experiment, indicating that removal of fucose impacts the way in which the receptor gains access to the IgG1. The observed differences in H/DX were more pronounced with increasing deuterium exposure, supporting the idea that the changes are more likely due to protein dynamics instead of a result of interaction surfaces (48, 49). If the change were a result of occlusion or creation of a protected binding interface involving amide hydrogens that were solvent-exposed, the H/DX differences observed should be maintained throughout the entire H/DX experiment encompassing all time points.

Overall, we conclude that the PTMs investigated in this work only partially influence and change the conformation and conformational dynamics of IgG1. Some modifications are likely transmitted to receptor binding via conformational changes, and others are likely not. On the basis of the findings described above and in combination with previous studies, it seems most possible that the extended glycan structures mediate the binding with FcγRIIIa by increasing the plasticity of the CH2 domain, which is communicated through residues 243–247 and additionally through residues 279–301 for the fucose-depleted form. The IgG1-FcγRIIIa interaction in solution may involve more than just regions at the IgG1 hinge and upper CH2 domain contacts (Fig. 6*A*), as indicated by changes in deuterium exchange, and could be influenced by residues in the CH1 domain (Fig. 6*C*).

Finally, we believe our results, along with earlier work (22), highlight again the amazing potential of H/DX MS in understanding monoclonal antibody higher order structure and structural dynamics (50). These H/DX MS experiments required only microgram quantities of protein and were completed in a relatively short period of time (days). In terms of beginning to understand the structural consequences of protein modifications, H/DX MS has great capabilities. The changes we observed went undetected by other biophysical methods, and such is likely the case for many other systems in which conformational changes are linked to function. Therefore, we strongly believe that H/DX MS should find its way into the toolbox of anyone wishing to understand how structure and dynamics are influenced by outside forces (drug binding, protein-protein interaction, etc.) and particularly by the biopharmaceutical industry in studies where comparability, stability, and general structural analysis are of great importance.

REFERENCES

1. Walsh, C. T. (2006) *Posttranslational Modification of Proteins: Expanding Nature's Inventory*, 1st Ed., Roberts and Co. Publishers, Greenwood Village, CO

2. Johnson, L. N., and Barford, D. (1993) The effects of phosphorylation on the structure and function of proteins. *Annu. Rev. Biophys. Biomol. Struct.* **22,** 199–232

3. Carter, P. J. (2006) Potent antibody therapeutics by design. *Nat. Rev. Immunol.* **6,** 343–357

4. Saphire, E. O., Parren, P. W., Pantophlet, R., Zwick, M. B., Morris, G. M., Rudd, P. M., Dwek, R. A., Stanfield, R. L., Burton, D. R., and Wilson, I. A. (2001) Crystal structure of a neutralizing human IGG against HIV-1: a template for vaccine design. *Science* **293,** 1155–1159

5. Garber, E., and Demarest, S. J. (2007) A broad range of Fab stabilities within a host of therapeutic IgGs. *Biochem. Biophys. Res. Commun.* **355,** 751–757

6. Jefferis, R. (2009) Glycosylation as a strategy to improve antibody-based therapeutics. *Nat. Rev. Drug Discov.* **8,** 226–234

7. Walsh, G., and Jefferis, R. (2006) Post-translational modifications in the context of therapeutic proteins. *Nat. Biotechnol.* **24,** 1241–1252

8. Walsh, C. T., Garneau-Tsodikova, S., and Gatto, G. J., Jr. (2005) Protein posttranslational modifications: the chemistry of proteome diversifications. *Angew. Chem. Int. Ed. Engl.* **44,** 7342–7372

9. Aebersold, R., and Mann, M. (2003) Mass spectrometry-based proteomics. *Nature* **422,** 198–207

10. Bertolotti-Ciarlet, A., Wang, W., Lownes, R., Pristatsky, P., Fang, Y., Mc-Kelvey, T., Li, Y., Li, Y., Drummond, J., Prueksaritanont, T., and Vlasak, J. (2009) Impact of methionine oxidation on the binding of human IgG1 to Fc Rn and Fc gamma receptors. *Mol. Immunol.* **46,** 1878–1882

11. Robison, A. J., Winder, D. G., Colbran, R. J., and Bartlett, R. K. (2007) Oxidation of calmodulin alters activation and regulation of CaMKII. *Biochem. Biophys. Res. Commun.* **356,** 97–101

12. Silva, M. M., Lamarre, B., Cerasoli, E., Rakowska, P., Hills, A., Bailey, M. J., Wheeler, J. X., Burns, C. J., Gaines-Das, R. E., Jones, C., and Robinson, C. J. (2008) Physicochemical and biological assays for quality control of biopharmaceuticals: interferon alpha-2 case study. *Biologicals* **36,** 383–392

13. Waak, J., Weber, S. S., Görner, K., Schall, C., Ichijo, H., Stehle, T., and Kahle, P. J. (2009) Oxidizable residues mediating protein stability and cytoprotective interaction of DJ-1 with apoptosis signal-regulating kinase 1. *J. Biol. Chem.* **284,** 14245–14257

14. Jefferis, R., Lund, J., and Pound, J. D. (1998) IgG-Fc-mediated effector functions: molecular definition of interaction sites for effector ligands and the role of glycosylation. *Immunol. Rev.* **163,** 59–76

15. Arnold, J. N., Wormald, M. R., Sim, R. B., Rudd, P. M., and Dwek, R. A. (2007) The impact of glycosylation on the biological function and structure of human immunoglobulins. *Annu. Rev. Immunol.* **25,** 21–50

16. Mimura, Y., Church, S., Ghirlando, R., Ashton, P. R., Dong, S., Goodall, M., Lund, J., and Jefferis, R. (2000) The influence of glycosylation on the thermal stability and effector function expression of human IgG1-Fc: properties of a series of truncated glycoforms. *Mol. Immunol.* **37,** 697–706

17. Yamaguchi, Y., Nishimura, M., Nagano, M., Yagi, H., Sasakawa, H., Uchida, K., Shitara, K., and Kato, K. (2006) Glycoform-dependent conformational alteration of the Fc region of human immunoglobulin G1 as revealed by NMR spectroscopy. *Biochim. Biophys. Acta* **1760,** 693–700

18. Nölting, B. (2006) *Methods in Modern Biophysics*, 2nd Ed., Springer, New York

19. Chruszcz, M., Wlodawer, A., and Minor, W. (2008) Determination of protein structures—a series of fortunate events. *Biophys. J.* **95,** 1–9

20. Foster, M. P., McElroy, C. A., and Amero, C. D. (2007) Solution NMR of large molecules and assemblies. *Biochemistry* **46,** 331–340

21. Sprangers, R., Velyvis, A., and Kay, L. E. (2007) Solution NMR of supramolecular complexes: providing new insights into function. *Nat. Methods* **4,** 697–703

22. Houde, D., Arndt, J., Domeier, W., Berkowitz, S., and Engen, J. R. (2009) Characterization of IgG1 conformation and conformational dynamics by hydrogen/deuterium exchange mass spectrometry. *Anal. Chem.* **81,** 2644–2651

23. Warnock, D., Bai, X., Autote, K., Gonzales, J., Kinealy, K., Yan, B., Qian, J., Stevenson, T., Zopf, D., and Bayer, R. J. (2005) In vitro galactosylation of human IgG at 1 kg scale using recombinant galactosyltransferase. *Biotechnol. Bioeng.* **92,** 831–842

24. Houde, D., Kauppinen, P., Mhatre, R., and Lyubarskaya, Y. (2006) Determination of protein oxidation by mass spectrometry and method transfer to quality control. *J. Chromatogr. A* **1123,** 189–198

25. Pace, C. N., Vajdos, F., Fee, L., Grimsley, G., and Gray, T. (1995) How to measure and predict the molar absorption coefficient of a protein. *Protein Sci.* **4,** 2411–2423

26. Glickman, J. F., Wu, X., Mercuri, R., Illy, C., Bowen, B. R., He, Y., and Sills, M. (2002) A comparison of ALPHAScreen, TR-FRET, and TRF as assay methods for FXR nuclear receptors. *J. Biomol. Screen.* **7,** 3–10

27. Wales, T. E., Fadgen, K. E., Gerhardt, G. C., and Engen, J. R. (2008) High-speed and high-resolution UPLC separation at zero degrees Celsius. *Anal. Chem.* **80,** 6815–6820

28. Silva, J. C., Gorenstein, M. V., Li, G. Z., Vissers, J. P., and Geromanos, S. J. (2006) Absolute quantification of proteins by LCMSE: a virtue of parallel MS acquisition. *Mol. Cell. Proteomics* **5,** 144–156

29. Weis, D. D., Engen, J. R., and Kass, I. J. (2006) Semi-automated data processing of hydrogen exchange mass spectra using HX-Express. *J. Am. Soc. Mass Spectrom.* **17,** 1700–1703

30. Wales, T. E., and Engen, J. R. (2006) Hydrogen exchange mass spectrometry for the analysis of protein dynamics. *Mass Spectrom. Rev.* **25,** 158–170

31. Burkitt, W., and O'Connor, G. (2008) Assessment of the repeatability and reproducibility of hydrogen/deuterium exchange mass spectrometry measurements. *Rapid Commun. Mass Spectrom.* **22,** 3893–3901

32. Sondermann, P., Huber, R., Oosthuizen, V., and Jacob, U. (2000) The 3.2-A crystal structure of the human IgG1 Fc fragment-Fc gammaRIII complex. *Nature* **406,** 267–273

33. Boyd, P. N., Lines, A. C., and Patel, A. K. (1995) The effect of the removal of sialic acid, galactose and total carbohydrate on the functional activity of Campath-1H. *Mol. Immunol.* **32,** 1311–1318

34. Radaev, S., and Sun, P. (2002) Recognition of immunoglobulins by Fc-gamma receptors. *Mol. Immunol.* **38,** 1073–1083

35. Mimura, Y., Sondermann, P., Ghirlando, R., Lund, J., Young, S. P., Goodall, M., and Jefferis, R. (2001) Role of oligosaccharide residues of IgG1-Fc in Fc gamma RIIb binding. *J. Biol. Chem.* **276,** 45539–45547

36. Okazaki, A., Shoji-Hosaka, E., Nakamura, K., Wakitani, M., Uchida, K., Kakita, S., Tsumoto, K., Kumagai, I., and Shitara, K. (2004) Fucose depletion from human IgG1 oligosaccharide enhances binding enthalpy and association rate between IgG1 and FcgammaRIIIa. *J. Mol. Biol.* **336,** 1239–1249

37. Satoh, M., Iida, S., and Shitara, K. (2006) Non-fucosylated therapeutic antibodies as next-generation therapeutic antibodies. *Expert Opin. Biol. Ther.* **6,** 1161–1173

38. Krapp, S., Mimura, Y., Jefferis, R., Huber, R., and Sondermann, P. (2003) Structural analysis of human IgG-Fc glycoforms reveals a correlation between glycosylation and structural integrity. *J. Mol. Biol.* **325,** 979–989

39. Ionescu, R. M., Vlasak, J., Price, C., and Kirchmeier, M. (2008) Contribution of variable domains to the stability of humanized IgG1 monoclonal antibodies. *J. Pharm. Sci.* **97,** 1414–1426

40. Liu, D., Ren, D., Huang, H., Dankberg, J., Rosenfeld, R., Cocco, M. J., Li, L., Brems, D. N., and Remmele, R. L., Jr. (2008) Structure and stability changes of human IgG1 Fc as a consequence of methionine oxidation. *Biochemistry* **47,** 5088–5100

41. Smith, D. L., Deng, Y., and Zhang, Z. (1997) Probing the non-covalent

structure of proteins by amide hydrogen exchange and mass spectrometry. *J. Mass Spectrom.* **32,** 135–146

42. Engen, J. R. (2003) Analysis of protein complexes with hydrogen exchange and mass spectrometry. *Analyst* **128,** 623–628

43. Radaev, S., Motyka, S., Fridman, W. H., Sautes-Fridman, C., and Sun, P. D. (2001) The structure of a human type III Fcgamma receptor in complex with Fc. *J. Biol. Chem.* **276,** 16469–16477

44. Deisenhofer, J. (1981) Crystallographic refinement and atomic models of a human Fc fragment and its complex with fragment B of protein A from Staphylococcus aureus at 2.9- and 2.8-A resolution. *Biochemistry* **20,** 2361–2370

45. Wormald, M. R., Rudd, P. M., Harvey, D. J., Chang, S. C., Scragg, I. G., and Dwek, R. A. (1997) Variations in oligosaccharide-protein interactions in immunoglobulin G determine the site-specific glycosylation profiles and modulate the dynamic motion of the Fc oligosaccharides. *Biochemistry* **36,** 1370–1380

46. Matsumiya, S., Yamaguchi, Y., Saito, J., Nagano, M., Sasakawa, H., Otaki, S., Satoh, M., Shitara, K., and Kato, K. (2007) Structural comparison of fucosylated and nonfucosylated Fc fragments of human immunoglobulin G1. *J. Mol. Biol.* **368,** 767–779

47. Shoemaker, B. A., Portman, J. J., and Wolynes, P. G. (2000) Speeding molecular recognition by using the folding funnel: the fly-casting mechanism. *Proc. Natl. Acad. Sci. U.S.A.* **97,** 8868–8873

48. Dharmasiri, K., and Smith, D. L. (1996) Mass spectrometric determination of isotopic exchange rates of amide hydrogens located on the surfaces of proteins. *Anal. Chem.* **68,** 2340–2344

49. Mandell, J. G., Falick, A. M., and Komives, E. A. (1998) Identification of protein-protein interfaces by decreased amide proton solvent accessibility. *Proc. Natl. Acad. Sci. U.S.A.* **95,** 14705–14710

50. Engen, J. R. (2009) Analysis of protein conformation and dynamics by hydrogen/deuterium exchange MS. *Anal. Chem.* **81,** 7870–7875

51. Krieger, E., Koraimann, G., and Vriend, G. (2002) Increasing the precision of comparative models with YASARA NOVA—a self-parameterizing force field. *Proteins* **47,** 393–402